

Chandra ACIS-S X-ray Imaging Spectroscopy of Comet 103P/Hartley 2

C.M. Lisse¹, D.J. Christian², S.J. Wolk³, D. Bodewits⁴, K. Dennerl⁵, M.R. Combi⁶, S.T. Lepri⁶, and T.H. Zurbuchen⁶
¹JHU-APL, 11100 Johns Hopkins Road, Laurel, MD 20723 carey.lisse@jhuapl.edu ²CSUN ³CXC, Harvard-SAO
⁴University of Maryland ⁵Max-Planck-Institut für extraterrestrische Physik ⁶University of Michigan

1. Introduction

Cometary X-ray emission, first discovered in 1996 and now observed in over 20 comets [1-3], has been shown to be caused by charge exchange reactions between highly charged solar wind minor ions (~0.1% of all solar wind ions) and neutral gas species emitted by the nucleus into the cometary coma [2, 4-8]. The emission originates predominantly from the sunward hemisphere of the neutral coma, in a 3-dimensional SW-coma plasma structure projected on the sky. In the ideal collisionally thick case for a highly active comet with $Q_{H2O} > 10^{30}$ mol/sec, where all incoming solar wind ions interact with cometary neutrals, what is seen is akin to a parabola of revolution with the comet at the focus, emitting x-ray photons at energies characteristic of atomic cascades from excited hydrogen-like and helium-like C, N, O, and Ne and a luminosity proportional to the solar wind ion flux density.

The solar wind has large-scale structure relating to the very different corona environments at the equator and pole of the Sun: the typical low-latitude solar wind is relatively dense, slow moving ($v = 200$ to 300 km s $^{-1}$), and of high temperature ($\sim 2 \times 10^6$ K), while the high-latitude polar wind is less dense and cooler ($\sim 1 \times 10^6$ K) but moving at higher average speeds ($v > 400$ km s $^{-1}$). These differences cause detectable differences in observed cometary X-ray spectra [8-10], allowing mapping of the heliospheric solar wind structure using comets as “standard candles”, once cometary activity emission effects are understood [11]. E.g., limitations of the emission region to the volume of the neutral coma available to the solar wind are predicted, with evidence in the morphology and size of the emission region [12, 13]. Modulation of the X-ray signal due to variability of the neutral coma density also occurs for systems that are collisionally thin [14].

To date, the best-observed comets in the X-ray have been comets with high coma “activity” (i.e., rate of sublimation of volatile ices into neutral gas species in the gravitationally unbound atmosphere surrounding the nucleus) and close Earth approachers, allowing accurate measurement of the solar wind state using the fleet of near-Earth monitoring spacecraft. The highly favorable, very close perigee passage

($\Delta_{min} = 0.104$ AU) of the short orbital period, Jupiter family comet 103P/Hartley 2 in late October-November 2010, coinciding with the *in situ* flyby through the comet’s coma of the EPOXI spacecraft, provided a unique opportunity to study in-depth the nature of cometary x-ray emission, the nature of the cometary plasma environment, and the behavior of the solar wind using what has turned out to be the second faintest x-ray comet ever detected.

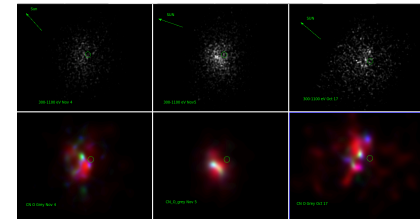


Figure 1 - Images of comet 103P/Hartley 2 taken on 17 Oct, 04 Nov, and 05 Nov 2010 by *Chandra* using the ACIS-S imaging spectrometer. **Upper tier** - 300-1100 eV x-ray photons. **Lower tier** - 3-color narrowband x-ray images taken in C & N (red), and O (green & blue) emission lines of comet, smoothed with a 5 pixel x 5 pixel gaussian filter. The green circle denotes the location of the nucleus and the green arrow the projected direction to the Sun in each image.

2. Observations

Comet 103P was observed by our team using *Chandra* X-ray Observatory (CXO) ACIS-S X-ray Imaging Spectroscopy in four separate pointings bracketing the EPOXI fly-by on 17 October 2010, 04 Nov (fly-by), 05 Nov and 16 Nov 2010. The observations were conducted from the Earth-orbiting CXO in the same manner as for our previous comet observations [3, 9, 14-17], with the comet’s nucleus near the aim-point in the ACIS S3 chip. No active guiding on the comet was attempted, and CXO was able to follow the comet using multiple pointings. With this method, the comet was centered on the S3 chip and allowed to drift across the FOV until the CXO pointing was updated to re-center the comet before it moved off the chip edge. The ACIS-S CCD array provides high resolution X-ray imaging with a plate scale of 0.5'' per pixel, an instantaneous field of view 8.3' x 8.3', and moderate resolution spectra ($\Delta E \sim 110$ eV FWHM, $\sigma_{Gaussian} \sim 50$ eV) in the 0.3 – 2.5 keV

(300 – 2500 eV) energy range. The circumstances of the observations were such that the heliocentric distance r_H (~ 1.07 AU) and elongation angle vs. the Sun ($119 \pm 5^\circ$) were nearly constant; the CXO-comet distance was monotonically increasing from Oct 17 through Nov 16th by almost a factor of 2; and the comet's neutral gas production rate was nearly constant at 9×10^{27} mol/sec except on Nov 4, when it was almost a factor of 50% lower.

3. Results

We found a total CXO x-ray luminosity on the order of 10^{-5} of the total optical luminosity, implying that x-ray emission is not a dominant term in the comet's energy budget. In fact, 103P's x-ray emission level was quite faint, an order of magnitude lower than usually found [16], and the second faintest comet ever observed in the x-ray [2]. X-ray images of the comet in the 300-1100 eV range containing photons created by CXE between highly stripped C, N, O, Ne, Fe and Si solar wind minor ions and neutral species in the comet's coma are presented in Figure 1.

The observed x-ray emission structures are highly non-uniform, and we conclude that 103P's coma was collisionally thin to charge exchange throughout the CXO monitoring period. Even though "hyperactive" i.e., a comet demonstrating sublimation rates supported by the entire nucleus surface, 103P was so small that the absolute Q_{H2O} ($5 - 9 \times 10^{27}$ mol/sec) was low enough that the average solar wind minor ion penetrated deeply into the coma before charge exchanging, and regions of x-ray emission track regions of highest coma neutral gas density, found mostly along variable, rotating jet structures.

In each of the 4 separate pointings, we obtained enough (3000 – 5000) counts to produce ACIS spectra with high signal-to-noise ratio, allowing model fits and derivation of the solar wind ion composition, flux density, and comet neutral gas abundance. The majority of prominent CXE emission lines can be attributed to the highly charged solar wind ions of C^{5+} , C^{6+} , N^{6+} , N^{7+} , O^{7+} , O^{8+} , Ne^{+9} and Ne^{+10} . Comparing the four different spectra in Figure 2, it can be seen that 103P interacted with different wind types. In particular the difference between Oct 17/Nov 4/Nov 5 and Nov 16 is striking. The decrease of the OVII peak around 0.57 keV requires a large decrease in the abundance of O^{+7} ions, and argues for a much lower coronal freeze-in temperature of the solar

wind on Nov 16, consistent with the ACE solar wind measurements for this date.

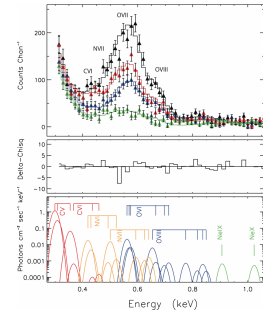


Figure 2 – Comet 103P CXO/ACIS S3 spectra & CXE fit for the Nov 05 (brightest) observation. **Top:** Observed spectra are shown (in order of intensity) for Nov 16 (green, bottom spectrum), Oct 17 (blue), Nov 04 (red), and Nov 05 (black, top spectrum). Overplotted are $\pm 1 \sigma$ error bars and the best fitting CXE models for each observations. **Middle:** Residuals of the CXE fit to the Nov 05 data. **Bottom:** Individual emission lines for a CXE model indicating the different lines and their strengths for the Nov 05 observation.

5. Acknowledgements

Support for this work was provided by the National Aeronautics and Space Administration through Chandra Award Number 12100872 issued by the Chandra X-ray Observatory Center, which is operated by the Smithsonian Astrophysical Observatory for and on behalf of the National Aeronautics Space Administration under contract NAS8-03060.

6. References

- [1] Lisse, C. M. *et al.*: *Science* **274**, 205, 1996
- [2] Dennerl, K., *et al.*: *Science* **277**, 1625, 1997
- [3] Bodewits, D., *et al.*: *Astron. Astroph.* **469**, 1183, 2007
- [4] Cravens, T.E. : *Geophys Res Lett* **24**, 105, 1997
- [5] Kharchenko & Dalgarno 2001, 2002
- [6] Krasnopolsky *et al.* 2002
- [7] Lisse, C. M., *et al.*: *Science* **292**, 1343, 2001
- [8] Lisse, C. M., *et al.*: *Icarus* **141**, 316, 1999
- [9] Beiersdorfer, P. *et al.*: *Science* **300**, 1558, 2003
- [10] Bodewits, D., *et al.*: *Astrophys. J.* **606**, L81, 2004
- [11] Lisse, C.M., T.E. Cravens, K. Dennerl: in *Comets II*, ed. M.C. Festou, H.A. Weaver, H.U. Keller, University of Arizona Press, 2004
- [12] Wegmann, R., *et al.*: *Astron. Astroph.* **428**, 647, 2004
- [13] Wegmann, R. & Dennerl, K., *Astron. Astroph.* **430**, L33, 2005
- [14] Lisse, C. M., *et al.*: *Astrophys. J.* **635**, 1329, 2005
- [15] Lisse, C.M., *et al.*: *Icarus* **190**, 391, 2007
- [16] Wolk, S.J., *et al.*: *Astrophys. J.* **694**, 1293, 2009
- [17] Christian, D.J., *et al.*: *Astrophys. J.* **187**, 447, 2010